Thermal and Mechanical Behavior of Amorphous and Semi-crystalline Poly(Vinylidene Fluoride)/Poly(Methyl Methacrylate) Blends

Jlidi Jarray,[1] *Fadhel Ben Cheikh Larbi*,[1] *Faustine Vanhulle*,[2] *André Dubault*,[1] *Jean Louis Halary**[2]

[1] Laboratoire de Physico-chimie des Matériaux Polymères, Institut Préparatoire aux Etudes Scientifiques et Techniques, BP51, 2070 La Marsa, Tunisia
[2] Laboratoire de Physico-chimie Structurale et Macromoléculaire (UMR 7615), Ecole Supérieure de Physique et Chimie Industrielles de la Ville de Paris, 10, rue Vauquelin, 75231 Paris cedex 05, France

Summary: Various PVDF/PMMA (poly(vinylidene fluoride)/poly(methyl methacrylate)) blends were selected for mechanical testing in compression. At low PVDF content (less than 50/50 w/w), the blends remain amorphous and PVDF and PMMA are fully miscible. In PVDF-richer blends, PVDF crystallizes in part, leading to a PMMA-enriched homogeneous amorphous phase. In this study, the degree of crystallinity was set at equilibrium by appropriate annealing of the samples before testing. Mechanical analysis was focused on the low deformation range, and especially on the yield region. Depending on the test temperature and blend composition, three types of response were identified, depending on whether plastic deformation is influenced: 1) by the PMMA secondary relaxation motions, 2) by the PVDF/PMMA glass transition motions, or 3) by the crystallite-constrained PVDF chains.

Keywords: blends, mechanical relaxation, plastic deformation, poly(methyl methacrylate), poly(vinylidene fluoride)

Introduction

In the 1970's, the PVDF/PMMA blends have been studied extensively, mainly in relation to PVDF piezoelectric properties.[1-7] Much attention has been paid to such problems as miscibility of the amorphous phase, crystallization of PVDF in various allotropic phases, and molecular origin of the PVDF/PMMA interactions. Moreover, blending with PMMA was described as an original way to force PVDF to crystallize into the piezoelectric phase, which is thermodynamically unstable in pure material.[8] More recently, the interest for the PVDF/PMMA was re-actualized, because of some potential applications as coatings and in building trade. In this new context, many studies was devoted to the characterization of the mechanical properties of the blends. The purpose of the present publication is to focus on the small deformations in compression and to analyze the yield region as a function of blend composition and, in turn, degree of crystallinity of the samples. As the strains are systematically lower than about 0.1, the PVDF crystallites, whenever they exist, are supposed not to deform. Therefore, the observed plastic deformation is expected just to depend on the

 DOI: 10.1002/masy.200350810

characteristics of the PVDF/PMMA amorphous phase. Emphasis will be put on chain mobility, according to the methodology already proposed for PMMA[9] and many other amorphous polymeric materials.[10-14]

Experimental

Materials. The PMMA used in this study was an amorphous polymer of high molecular weight, prepared by conventional free radical polymerization. Its glass transition temperature, as determined by DSC at heating rate of 10K/min, was Tg_A = 110°C. The grade of used PVDF presented a melt viscosity of 830 Pa.s at 230°C, a glass transition temperature Tg_F = -40°C, a melting temperature Tm_F = 165-172°C and a maximum degree of crystallinity of about 50%. Both materials were kindly provided by ATOFINA.

Blending procedure. Homogeneous dilute solutions were prepared by dissolving 5w% of polymeric materials in dimethylformamide, under continuous stirring at 50°C for 24 h. Then, PVDF and PMMA were co-precipitated, by pouring the solution drop by drop into a large excess of water. Finally, the polymeric powder was dried at 100°C for 15 h in a vacuum oven. Blends prepared in this way covered the composition range from 10/90 to 90/10 w/w.

Samples for mechanical testing. The dry powder was compression molded in the form of sheets (200*200*3 mm^3) under press, at 200°C for 30 mn. Then, small bars (6*3*3 mm^3) were cut from the sheets by using a diamond saw. As justified in the results and discussion section, the bars of composition likely to crystallize (i.e. containing at least 50 w% of PVDF) were subjected to an annealing step of 60 h at 150°C, prior to mechanical testing.

DSC experiments. Measurements were performed on a modulated differential scanning calorimeter (DSC universal v3.0G, from TA Instruments), by using a heating rate of 10K/min and a 1Hz sinusoidal modulation with an amplitude of ± 1°C. The characteristic temperatures Tg and Tm were taken at the onset of the heat capacity jump and at the extremum of the melting peak, respectively, both being relative to the in-phase signal.

Stress-strain curves. Mechanical measurements were performed on a MTS-810 testing system, equipped with an isothermal chamber and non-lubrificated plates. The experiments covered the temperature range from –50°C to Tg – 20 K. The strain rate was always equal to $2.10^{-3}s^{-1}$. As a first approximation, nominal stress was considered instead of the true stress, since the strains under inspection are quite low.

Results and Discussion

DSC Data

Glass transition temperature of the amorphous blends. As expected from earlier studies,[7] the blends containing up to 40w% PVDF are totally amorphous and their DSC traces just show a heat capacity jump at Tg. Dependence of Tg_{blend} on composition is shown in Figure 1. Its asymmetric character results from the occurrence of specific interactions between the blend components. It can be accounted for by using a modified Fox equation of the type :

$$\frac{w_A + kw_F}{Tg_{blend}} = \frac{w_A}{Tg_A} + k\frac{w_F}{Tg_F} \qquad (1)$$

where w_A and w_F are the weight fractions of PMMA and PVDF, respectively, and k is an empirical fit constant.

DSC traces of the blend PVDF/PMMA 50/50. For the sample rapidly quenched from the melt (without further annealing), the thermogram shows a Tg_{blend} around 40°C (in agreement with Figure 1), and then an exothermic peak around 140°C. This indicates that some PVDF crystallization occurs during the temperature scan. In order to set the degree of crystallinity at equilibrium, the samples were annealed at 150°C for various times until a plateau is reached. Reasonable estimates of PVDF crystalline weight fraction, y, were deduced from the melting peak areas. It turns out (Figure 2) that the critical annealing time was around 50 h, and that further DSC scan did not reveal the presence of any crystallization peak. In turn, Tg_{blend} was shown to increase with annealing time until a constant value is also reached for 50 h (Figure 3). This feature is indicative of the enrichment of the amorphous phase in PMMA, as the result of gradual PDVF crystallization.

DSC data for the other semi-crystalline PVDF/PMMA blends. As the blend 50/50 is the less crystallizable material of the series, it is obvious that the PVDF-richer blends get *a fortiori* the equilibrium degree of crystallinity after the annealing step (60 h at 150°C).

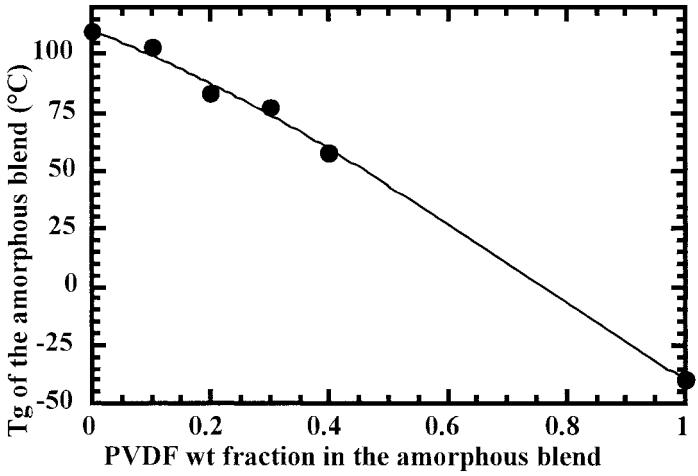

Fig. 1. Glass transition temperature versus composition for the amorphous blends (circles: experimental values; solid line : best fit from Equation (1) with k = 0.76).

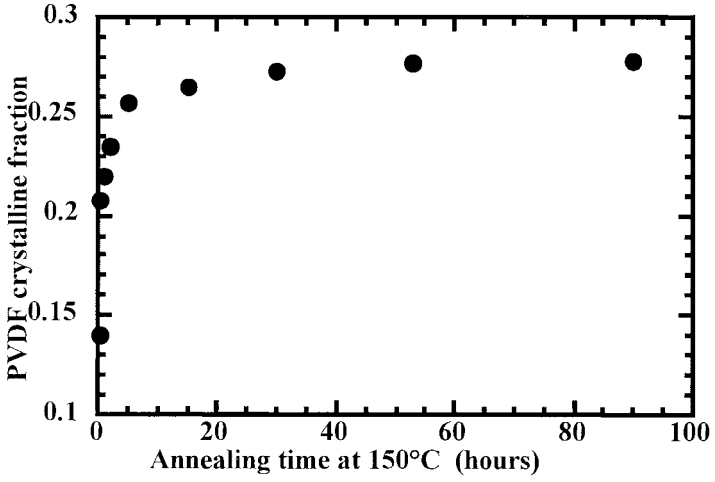

Fig. 2. PVDF crystalline fraction versus annealing time at 150°C for PVDF/PMMA 50/50.

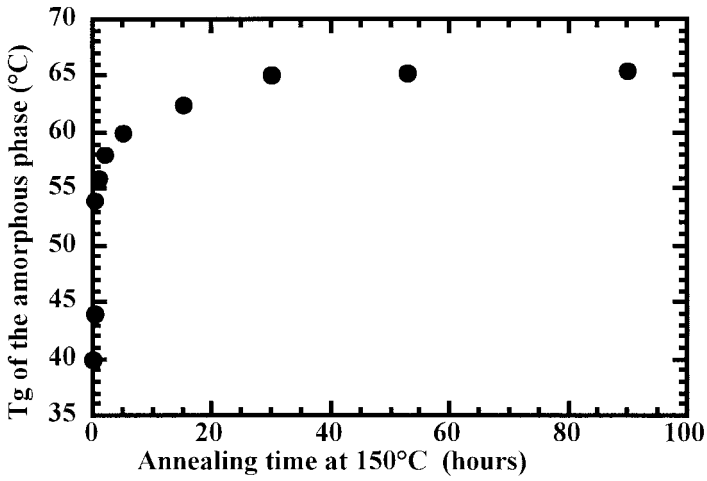

Fig. 3. PVDF/PMMA 50/50: effect of the annealing time (at 150°C) on the glass transition temperature of the amorphous phase.

In Figure 4, the PVDF crystalline fraction, y, (in weight) is plotted as a function of the overall percentage of PVDF in the blend. This quantity strongly increases with increasing PVDF amount in the blend. This behavior is consistent with the parallel increase in blend density. In addition, Tm also increases (Figure 5), suggesting that the crystallites grow in size and degree of perfection with increasing percentage of PVDF in the blend.[3] Consideration of the amorphous phase Tg (Figure 6) shows that this quantity levels off for the highest PVDF amounts. As shown by simple calculations, this result cannot be uniquely explained by the PMMA enrichment of the amorphous phase, which accompanies PVDF cristallization. To this end, let us first calculate the PVDF weight fraction, w_{Fa}, in the amorphous phase from the crystallinity data thanks to the relation :

$$W_{Fa} = \frac{W_F (1 - y)}{1 - yW_F} \qquad (2)$$

and then deduce the calculated value of Tg_{blend} from equation 1 (with k = 0.4842). As shown in Table 1, the values derived from the mixing law deviate from the experimental measurements, and the PVDF-richest blends present the largest deviations. These apparent discrepancies originate probably from the rigidification of those of the amorphous PVDF skeletal bonds which are located along the chain in the vicinity of bonds involved in the crystallites. The more crystalline the blend, the more numerous the amorphous bonds which are constrained by the crystalline phase, and the higher the Tg_{blend}.

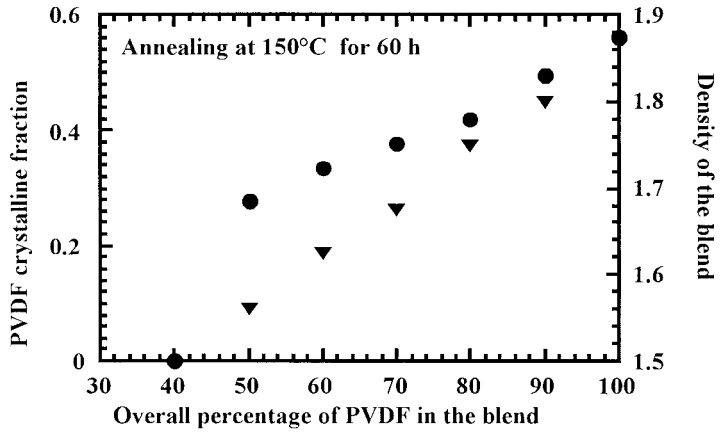

Fig. 4. PVDF crystalline fraction (circles) and density of the blend (triangles) versus blend composition.

Table 1. Thermal properties of semi-crystalline PVDF/PMMA blends.

PVDF/PMMA	w_F	w_{Fa}	Experimental Tg_{blend} °C	Calculated Tg_{blend} °C
50/50	0.50	0.42	66	58
60/40	0.60	0.50	54	45
70/30	0.70	0.60	45	27
80/20	0.80	0.70	54	12
90/10	0.90	0.82	53	-7

Analysis of the Stress-strain Curves

General features. Figure 7 shows the shape of typical stress-strain curves covering the entire range of blend composition, namely : a) the PMMA-richest blend 10/90, b) the PMMA-poorest amorphous blend 40/60, and the PVDF-richest blend 90/10. For the amorphous blends, the curves a) and b) have in common to present a usual profile, including an initial linear part, typical of the elastic response, then a curvature corresponding to the inelastic response before the yield point is attained at the maximum stress σ_y. They distinguish from each other by the stress changes after the yield point.

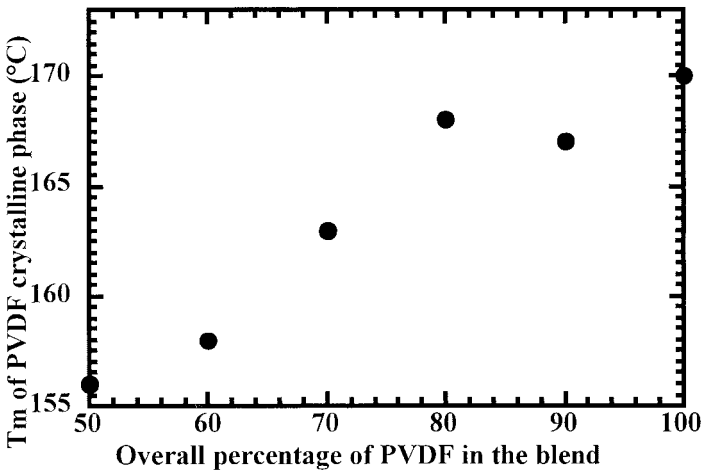

Fig. 5. Melting temperature of the PVDF crystalline phase versus blend composition for the semi-crystalline blends.

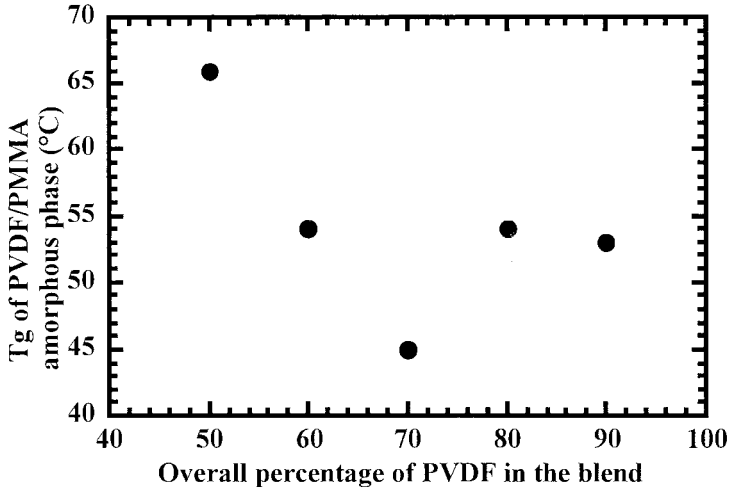

Fig. 6. Glass transition temperature of the amorphous phase versus blend composition for the semi-crystalline blends.

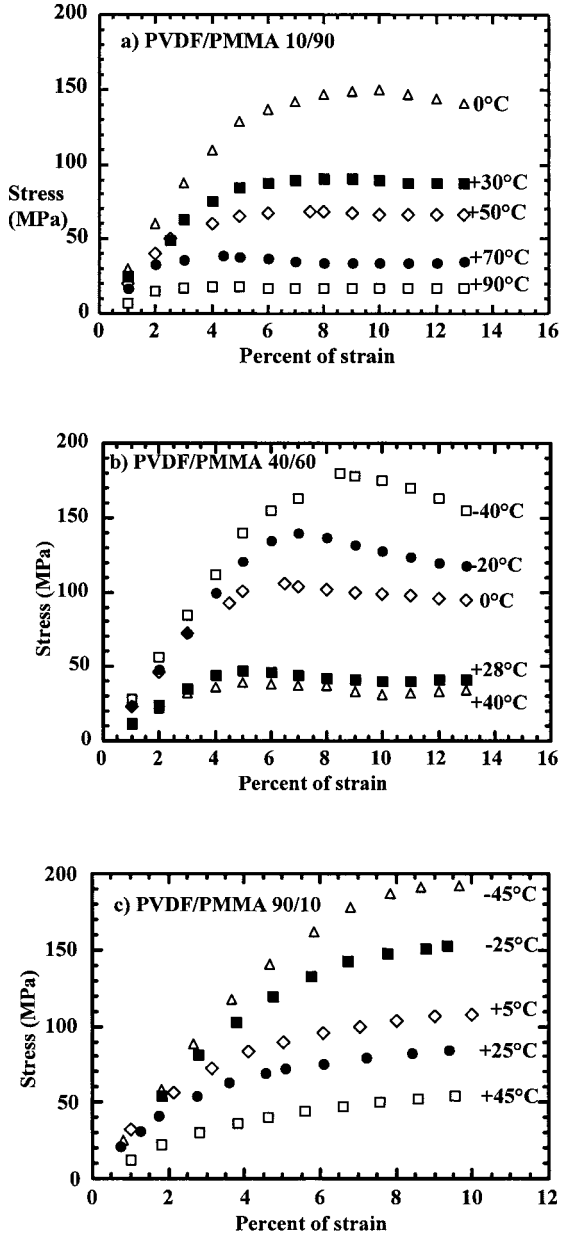

Fig. 7. Stress-strain curves for three typical blend compositions at various test temperatures.

A marked softening is observed on the curve b) until a plateau is reached, characterized by the plastic flow stress, σ_{pf}. On the other hand, almost no strain softening shows up on the curves a). For the semi-crystalline materials (curves c)), both yield point and strain softening are hidden by the occurrence of a strong strain hardening, which develops very rapidly at the end of the domain of elastic response. Conventionally, a 'pseudo-yield' can be defined, as sketched in Figure 8.

Influence of chain mobility on the observed behavior. In the case of amorphous materials, it is recognized that the plastic deformation events are closely related to the chain motions.[15-18] Recent reports illustrated the suitability of such connections for various materials, including methyl methacrylate copolymers,[9,10] semi-aromatic polyamides,[11,12] epoxy resins[13] and polystyrene/poly(phenylene oxide) compatible blends.[14]

A simple way to visualize the situation encountered for the PVDF/PMMA amorphous blends is to calculate first the mechanical energy, W_y , required to attain the yield point, which is approximately given by (see Figure 8):

$$W_y = \sigma_y\left(\varepsilon_y - \frac{\varepsilon_{ey}}{2}\right) \qquad (3)$$

and then to follow the decrease of W_y with increasing temperature.

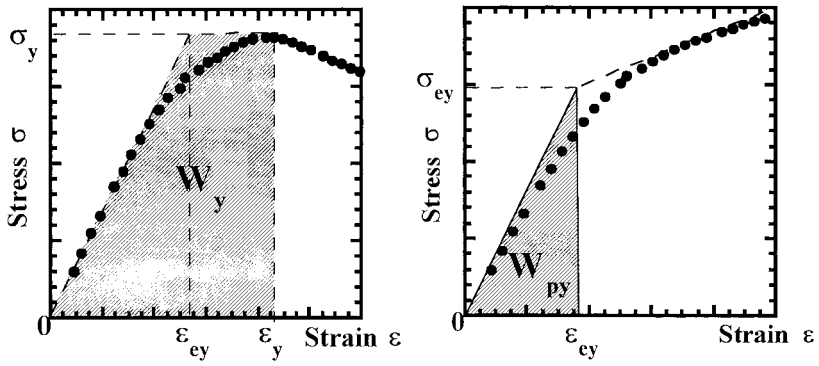

Fig. 8. Evolution of the mechanical energy to yield for the two types of stress-strain curves (left: with softening; right: with hardening).

As shown in Figure 9, the plots of W_y versus test temperature reveal the occurrence of two well-separated profiles. In the high temperature range, W_y extapolates linearly to zero at a temperature close to Tg_{blend}, just meaning that plastic flow becomes there a spontaneous, thermally activated process. Interestingly, in the lower temperature range, another linear

profile is observed. In that case, W_y extrapolates to zero in the temperature range of the PMMA β relaxation,[9] putting emphasis on the influence of the β motions on the deformation process. These trends are summarized in Figure 10.

The same procedure holds for the semi-crystalline blends, provided W_y is replaced, in the absence of true yield point, by W_{py} calculated as (see again Figure 8):

$$W_{py} = \frac{\sigma_{ey}\varepsilon_{ey}}{2} \qquad (4)$$

A unique straight line accounts for the temperature dependence of W_{py}, as illustrated in Figure 11 on the example of PVDF/PMMA 90/10. In this case, a residual value of σ_{ey} would be observed between Tg ad Tm as the result of the semi-crystalline character of the materials. However, W_{py} vanishes as σ_{ey} is extrapolated to zero, at a temperature very close to the experimental Tg_{blend}. This result holds whatever the semi-crystalline blend under consideration (Figure 12). The fact that yield properties are governed below Tα by the glass transition motions only can be understood very simply. Blend composition is such that the MMA units are rather scarce in these PVDF-rich blends. Therefore, PMMA secondary relaxation motions are not sufficiently numerous to generate the mobility microdomains which are likely to initiate the plastic deformation.

Molecular interpretation of strain softening and strain hardening. The shape of the PVDF/PMMA 10/90 stress-strain curves shown in Figure 7a resembles very much that reported in the literature for pure PMMA.[9] As a first approximation, it can be interpreted in the same way by neglecting the perturbation provoked by the scarce PVDF chains. Strain softening is very small in PMMA (and in PVDF/PMMA 10/90, too), because the β molecular motions responsible for yielding (so-called α-precursor β motions) are of same nature as the α motions responsible for plastic flow. On the other hand, strain softening enlarges as long as the blend PVDF content increases (see Figure 7b) because the PVDF chain segments contribute significantly to the α process. Therefore, PMMA β motions are no longer the precursors of the blend α motions and, in turn, the stress to be applied is much higher for yielding than for plastic flowing, as previously reported for MMA-based random copolymers including stiff units.[9] In other words, while comparing amorphous samples in isostructural conditions, difference in strain softening amplitude (σ_y - σ_{pf}) reflects the difference in the nature of the motions occurring at yield and plastic flow.

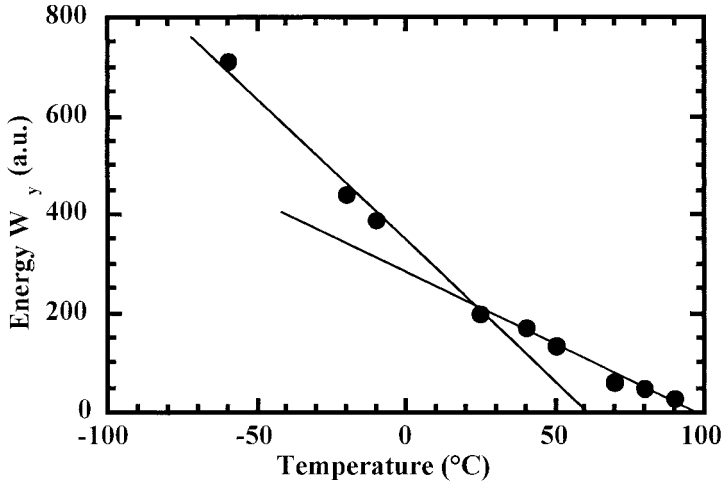

Fig. 9. Variation of the mechanical energy to yield, W_y, as a function of temperature for the amorphous 10/90 blend.

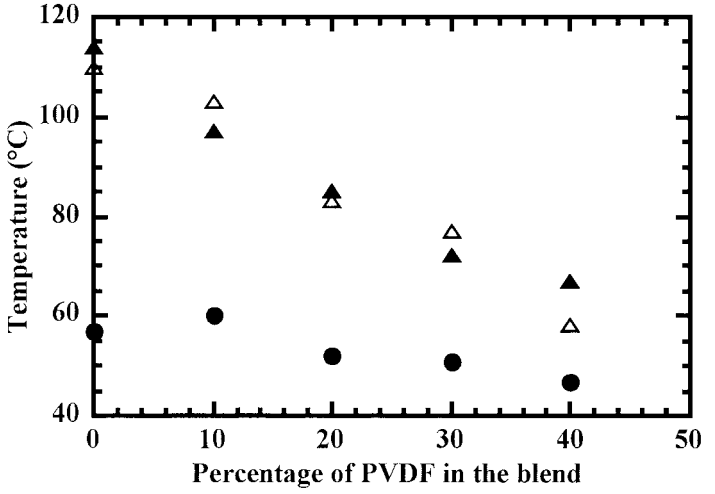

Fig. 10. Zero energy extrapolated temperatures as a function of amorphous blend composition (circles : low temperature regime; filled triangles : high temperature regime). The values of Tg_{blend} (open triangles) are also given for sake of comparison.

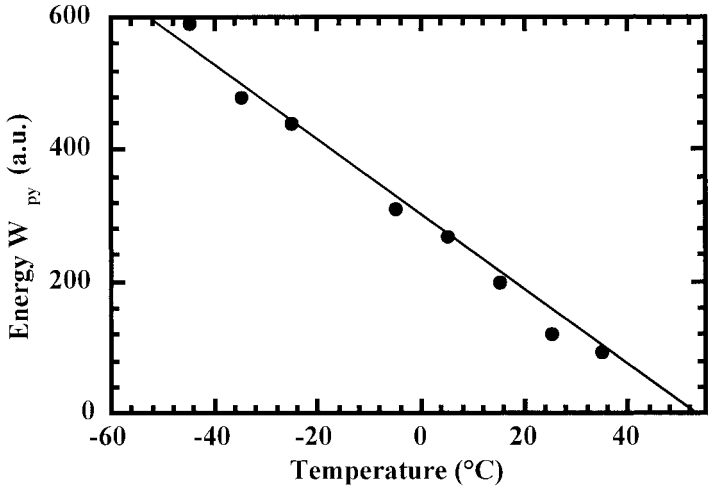

Fig. 11. Variation of the mechanical energy to yield, W_{py}, as a function of temperature for the semi-crystalline 90/10 blend.

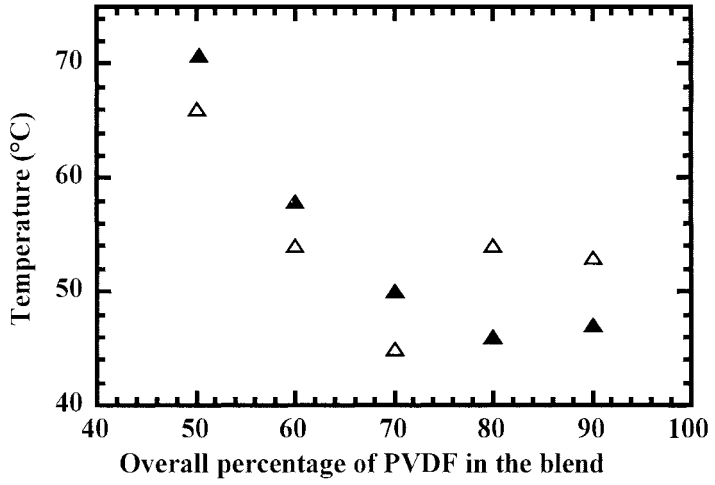

Fig. 12. Zero energy extrapolated temperatures (filled triangles) as a function of overall PVDF content for the semi-crystalline blends. The values of Tg_{blend} (open triangles) are also given for sake of comparison.

As far as the PVDF-rich semi-crystalline blends are concerned, the occurrence of the strain hardening phenomenon, which even conceals the true yield point (Figure 7c), is similar, from a phenomenological viewpoint, to what has been observed for nanosilica particle-filled PMMA.[19] In the latter case, a tentative explanation for the early hardening was that the PMMA chain deformation is limited by the vicinity of the undeformable silica particles. If so, some chains would reach very rapidly their limit of extensibility, and therefore an increased stress would be required to further deform the sample. On may suggest the same explanation for the PVDF amorphous segments constrained by the crystallites. Therefore, the higher the PVDF content in the blends, the more numerous the constrained segments and, in turn, the earlier the appearence of strain hardening. This finding is actually verified by comparing the behavior of the blends 50/50, 60/40, 70/30, 80/20 (stress-strain curves not shown here), and finally 90/10 (Figure 7c). It is supported by the above DSC data, which provide evidence for the presence of highly constrained PVDF chain segments in the amorphous phase.

Conclusions

For the amorphous PVDF/PMMA blends, a quantitative mixing law accounts for the variations of Tg as a function of blend composition, and the yield properties are influenced by the PMMA secondary relaxation motions in the lower temperature range and, at higher temperatures, by the blend α motions, which are the mechanical expression of the glass transition motions.

For the semi-crystalline PVDF/PMMA blends, the glass transition temperature of the amorphous phase, calculated from crystallinity data, deviates from the mixing law, as the expression of constrained chains. The higher the overall PVDF content, the larger the effect. Only a 'pseudo-yield' point is observed and the yield properties are governed by the Tg motions. As in PMMA nanohybrids, the crystallites reduce the limit extensibility of some PVDF segments in the amorphous phase, and a strong strain hardening effect is observed on the stress-strain curves.

WAXS and SAXS measurements are currently in progress with the aim of characterizing the PVDF crystalline phase in more details and getting further information on the constrained chains.

Acknowledgments

This study was supported by the 'Comité Mixte de Coopération Franco-Tunisienne' (CMCU) under contract No 01F1302. The authors would like to thank Dr François Beaume (ATOFINA, Serquigny, France) for kindly providing the PVDF and PMMA pure polymers and for his interest in this study. Thanks are also due to Mrs Amalia de Roffignac for her contribution to the experimental work.

[1] J.S. Noland, N.N.C. Hsu, R. Saxon, J.M. Schmitt, *Adv. Chem. Ser.* **1971**, *99*, 15.
[2] T. Nishi, T.T. Wang, *Macromolecules* **1975**, *8*, 909.
[3] T. Nishi, T.T. Wang, *Macromolecules* **1977**, *10*, 421.
[4] O. Faria, R.L. Moreira, *Polymer* **1999**, *40*, 4465.
[5] K. Saito, S. Miyata, T.T. Wang, Y.S. Jo, R. Chujo, *Macromolecules* **1986**, *19*, 2450.
[6] C. Léonard, J.L. Halary, L. Monnerie, D. Broussoux, B. Servet, F. Micheron, *Polymer, commun.* **1983**, *24*, 110.
[7] C. Léonard, J.L. Halary, L. Monnerie, F. Micheron, *Polym. Bull.* **1984**, *11*, 195.
[8] C. Léonard, J.L. Halary, L. Monnerie, *Macromolecules* **1988**, *21*, 2988.
[9] P. Tordjeman, L. Tézé, J.L. Halary, L. Monnerie, *Polym. Eng .Sci.* **1997**, *37*, 1631.
[10] L. Tézé, J.L. Halary, L. Monnerie, L. Canova, *Polymer* **1999**, *40*, 971.
[11] S. Choe, B. Brulé, L. Bisconti, J.L. Halary, L. Monnerie, *J. Polym. Sci., Polym. Phys. Ed.* **1999**, *37*, 1131.
[12] B. Brulé, L. Bisconti, J.L. Halary, L. Monnerie, *Polymer* **2001**, *42*, 9073.
[13] D. Rana, V. Sauvant, J.L. Halary, *J. Mater. Sci.* **2002**, in press.
[14] C. Creton, J.L. Halary, L. Monnerie, *Polymer* **1999**, *40*, 199.
[15] J.C. Bauwens, *J. Mater. Sci.* **1972**, *7*, 577.
[16] C.J. Bauwens-Crowet, *J. Mater. Sci.* **1973**, *8*, 968.
[17] J.M. Lefebvre, B. Escaig, *J. Mater. Sci.* **1985**, *20*, 438.
[18] J. Perez, "Physique et Mécanique des Polymères Amorphes", Tec. Doc. Lavoisier , Paris 1992.
[19] M. Mauger, Thesis of the University Pierre and Marie Curie (Paris VI), Dec. 2000.